Cooling and Near-equilibrium Dynamics of Atomic Gases Across the Superfluid-Mott Insulator Transition

Chen-Lung Hung, Xibo Zhang, Nathan Gemelke, and Cheng Chin
The James Franck Institute and Department of Physics,
The University of Chicago, Chicago, IL 60637, USA
(Dated: October 7, 2009)

We study near-equilibrium thermodynamics of bosonic atoms in a two-dimensional optical lattice by ramping up the lattice depth to convert a superfluid into an inhomogeneous mixture of superfluid and Mott insulator. Detailed study of *in situ* density profiles shows that, first, locally adiabatic ramps do not guarantee global thermal equilibrium. Indeed, full thermalization for typical parameters only occurs for experiment times which exceed one second. Secondly, ramping non-adiabatically to the Mott insulator regime can result in strong localized cooling at short times and global cooling once equilibrated. For an initial temperature estimated as 20 nK, we observe local temperatures as low as 1.5 nK, and a final global temperature of 9 nK. Possible cooling mechanisms include adiabatic decompression, modification of the density of states near the quantum critical regime, and the Joule-Thomson effect.

PACS numbers: 73.43.Nq,03.75.Kk,05.30.Jp,03.75.Lm

Ultracold atoms in optical lattices promise unique opportunities to simulate intriguing many-body models that are widely discussed in the context of condensed matter and many-body physics [1, 2]. In contrast to solid state materials, the complete knowledge and simplicity of the lattice potential, together with the tunability of atomic interactions, offer new prospects for a precise, quantitative comparison between calculations and measurements. Prominent examples are the superfluid-Mott insulator (SF-MI) transition of bosons in lattices [3], described by Bose-Hubbard model[4, 5], and the formation of Mott and band insulators in Fermi gases [6, 7], simulating the Fermi-Hubbard model [8]. The Bose-Hubbard model provides the simplest case to explore the quantum phase transition and quantum criticality [9], while the fermionic counterpart potentially holds the key to the mystery of high-Tc superconductivity. More novel phases in optical lattices have been proposed, independent of the existence of the condensed matter counterparts, and have provided new perspectives to explore exotic quantum phases. In many of these contexts, however, very low temperatures and new schemes to characterize the samples are required to proceed.

In optical lattice experiments, preparation and detection of the sample are subjects of active research. In most experiments, the lattice is introduced to the sample by gradually ramping up the lattice potential, and the sample is studied via the diffraction patterns of atoms in time-of-flight expansion. Issues have been raised and extensively studied on the adiabticity of the lattice ramping process [10–12], and the interpretation of the time-of-flight images [13, 15]. Here, complications arise from the existence of multiple phases in a harmonically trapped sample, and hydrodynamic behavior in free expansion. Despite these difficulties, many new ideas have also been proposed, and some implemented, to extract local and global information of atoms in the lattice [14, 16–18], and even to remove entropy for an inhomogeneously trapped sample [19, 20].

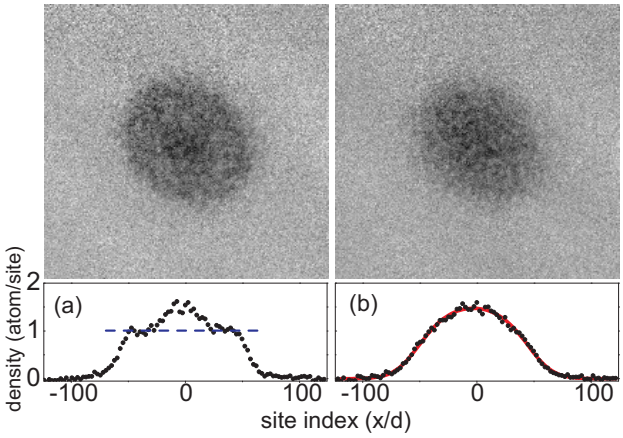

FIG. 1: Absorption images and averaged density cross section of $N = 12,000$ cesium atoms in 2D optical lattices after ramping up the lattice depth to V_f=13E_R. (a) shows the formation of plateau with unity occupancy (dotted line) after a 300 ms ramp (adiabaticity parameter $\alpha = \hbar\dot{t}/t^2 < 0.6$). (b) shows the profile after a 1200-ms ramp ($\alpha < 0.15$). Theoretical fit (solid line, see text) works well only in case (b). Images size= $(133\mu\text{m})^2 = (250 \text{ sites})^2$

In this letter, we address the above issues by studying the *in situ* density profiles of ultracold atomic gases in a two-dimensional optical lattice. We show that lattice ramps developed to ensure only local adiabaticity [11, 12] can yield samples far from global thermal equilibrium, which demands a much longer time scale, see Fig. 1. Though heating might generally be expected in such a non-equilibrium process, we show that nonadiabatic ramps can lead to significant cooling effects. From a finite-temperature density fit derived in the MI regime, we find that temperature can drop significantly in the central region of the sample.

We begin the experiment with a ^{133}Cs quantum gas

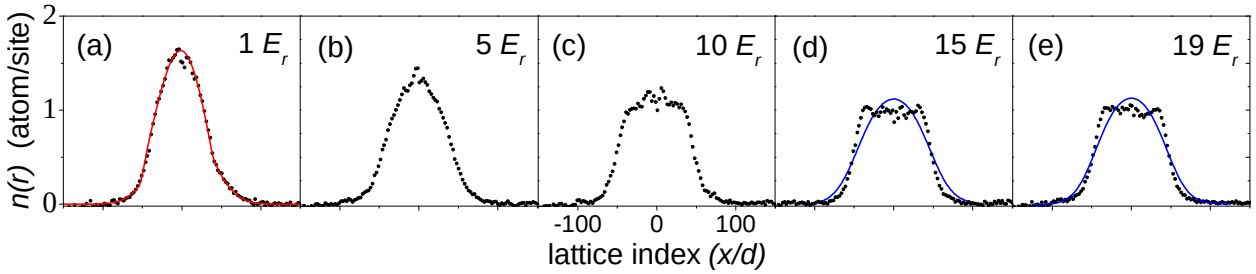

FIG. 2: Averaged density profiles of $N = 8,000$ cesium atoms measured immediately after the ramp with a time constant of $\tau_0 = 67$ ms and $\alpha < 0.95$. (a) and (b) are in superfluid regime. Bimodal fit (solid line) is shown for case (a). (c) is in the quantum phase transition regime $U/t = 15 \approx U/t|_c$. (d) ($U/t = 59$) and (e) ($U/t = 150$) are in the Mott insulator regime. The solid curves in (d) and (e) are fits based on Eq. 1 assuming a uniform temperature and chemical potential.

in a monolayer of a two-dimensional optical lattice. Details on the preparation of the quantum gas and optical lattice loading can be found in Ref. [21] and Ref. [14], respectively. In brief, a nearly pure Bose condensate is loaded into a 2D dipole trap, formed by two orthogonally crossed beams on the $x - y$ plane and a 1D vertical optical lattice which confines the whole sample in a single "pancake"-like lattice site [14]. The trap frequencies are $(\omega_x, \omega_y, \omega_z) = 2\pi \times (9.1, 12, 1500)$ Hz, and the sample temperature is $T = 20$ nK. The ratios $\hbar\omega/k_BT = (0.02, 0.03, 3.6)$ indicate the sample is two-dimensional.

A 2D optical lattice is formed by introducing retro-reflections of the crossed dipole beams, which add a square lattice potential of potential depth V with a lattice spacing of $d = 532$ nm and a very weak contribution to the envelope confinement as $\sqrt{\omega_x\omega_y}/2\pi = (1 + V/150E_r) \times 10.2$ Hz, where $E_r = k_B \times 64$ nK is the recoil energy. Care is taken to equalize lattice confinement in the x and y directions by balancing the trap frequencies to better than 2%. Tunneling t and on-site interaction U of atoms in the lattice are calculated numerically from band structure and Wannier wavefunctions in a homogeneous 2D lattice.

After the lattice is slowly turned on to $V = 0.4\ E_r$, we continue the ramp following $V(\tau) = V_f/(1 + e^{-\tau/\tau_0})$. Our standard ramping procedure uses $\tau_0 = 29$ ms and takes 250 ms to reach $V_f = 14\ E_r$, where we perform most of the analysis in this paper. Here, the system is in the MI regime with $U/t = 46$ and $t = k_B \times 0.5$ nK. This ramp has an adiabaticity parameter [12] $\alpha = \hbar\dot{t}/t^2 < 0.7$ throughout. This suggests local equilibrium of the system at the end of the ramp, as indicated by the time-of-flight images [11, 12].

In situ profiles of the sample are taken by 15 μs of absorption imaging. To avoid light assisted collision loss due to high local atomic density at high lattice depths, we switch off the 2D lattice 50 μs before the imaging, allowing atoms to expand and fill the area of one unit cell. The atomic density is measured with a spatial resolution of 1.3 μm using a long working distance (34 mm) commercial microscope objective. The strength and duration of the imaging pulse are chosen to keep the travel distance of atoms during imaging small compared to the depth of focus, while maintaining a good signal-to-noise ratio. Atomic occupation number n is calibrated using the density plateau feature [14]. Figure 2 shows the averaged line cut of the occupation number in different regimes based on a slow ramp with $\tau_0 = 67$ ms and $V_f = 19\ E_r$. The profiles are obtained by first correcting the ellipticity of the images, then averaging 45 line cuts with small angles of separation.

In weak optical lattices ($V < 5E_r$), the density profile near the central part bulges above the thermal tail, signifying the existence of superfluid. Here, the density profile can be described by a bimodal distribution, see Fig. 2 (a). Above $V = 5E_r$, the change of slope near $n = 1$ becomes apparent. At $V = 10\ E_r$, a clear density plateau forms near $n = 1$ while the central region of the cloud only slightly rises above $n = 1$, indicating the system just crosses the SF-MI transition; here, our calculation gives $U/t = 15$. The observation of the SF-MI transition here is consistent with previous experiment [22], as well as quantum Monte Carlo calculation, which predicts that a transition in a 2D lattice occurs at $U/t|_c = 16.74$ at the tip of the $n = 1$ Mott lobe [23]. Above $V = 10\ E_r$, density plateaus near $n = 1$ grow and eventually dominate the center of the sample. Detailed investigation on the critical regime and the phase diagram will be presented elsewhere.

Deep in the Mott insulator regime where tunneling is negligible $t \ll U, k_BT$, the spatial density of a thermalized sample can be compared to analytic models [17, 18]. Here, the mean occupation number can be written as

$$\bar{n} = \frac{\sum nP_n}{\sum P_n} = \frac{\sum ne^{-\beta[Un(n-1)/2-\mu n]}}{\sum e^{-\beta[Un(n-1)/2-\mu n]}}, \qquad (1)$$

where $P_n = \exp(-\beta H_n)$ is the probability for n particles to occupy one lattice site, H_n is the associated free energy (assuming $t = 0$), $\beta = 1/k_BT$, and μ is the local chemical potential.

For samples in a weak trap with potential energy $V_{ex}(r)$, we assume a local density approximation $\mu(r) = \mu_c - V_{ex}(r)$, and thus turn the above equation into a

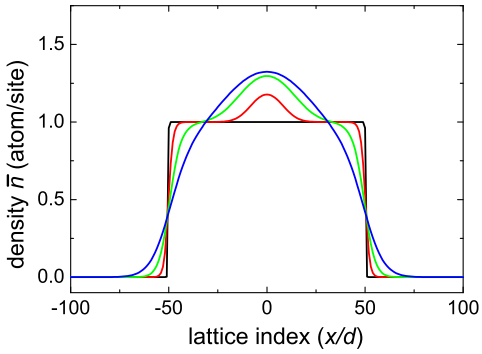

FIG. 3: Density profiles in the deep Mott insulator regime. The profiles are calculated based on Eq. 1 and parameters relevant to our experiment: $U = k_B \times 24$ nK, $N = 8,000$ and $V_{ex}(r) = k_B \times 9.0$ pK$(r/d)^2$. Temperatures are 0.1 nK (black), 1 nK (red), 2.5 nK (green) and 5 nK (blue).

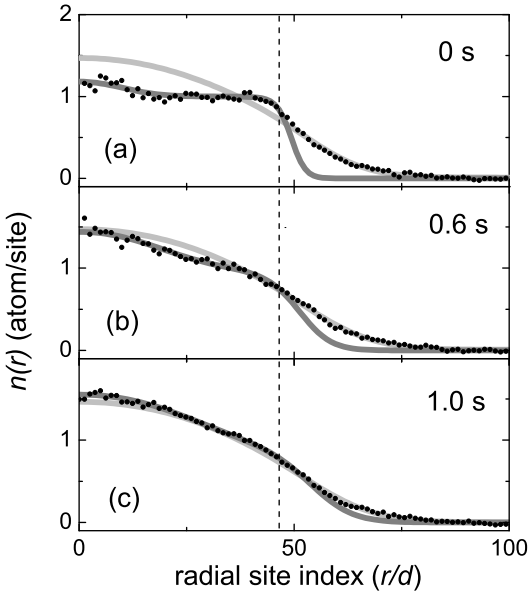

FIG. 4: Evolution of the density profiles after ramping into the Mott insulator regime ($N = 1.0 \times 10^4$, $V_f = 14\ E_r$, standard ramping procedure). Independent fits to the inner part $r < 45d$ (dark gray) and outer part $r > 45d$ (light gray) of the profiles yield temperatures T_1 (inner) and T_2 (outer); (a) immediately after the ramp, we have $(T_1, T_2) = (1.5, 7.9)$ nK; (b) after 0.6 s hold time, $(T_1, T_2) = (3.5, 8.4)$ nK; (c) after 1.0 s hold time, $(T_1, T_2) = (5.3, 8.7)$ nK. The vertical dashed line separates the two fitting regimes.

density fit $\bar{n}(r; T, \mu_c)$ with temperature T and chemical potential at the trap center μ_c as two free parameters. Illustration of the density fit function is shown in Fig. 3 based on parameters close to our experiment. The calculation shows that the plateau feature is clear only at temperatures equal or below 2.5 nK and quickly disappear approaching 5 nK or higher. This conclusion is consistent with Ref. [18, 24].

This density function fits very well the profiles of thermalized samples prepared either by an extremely slow ramp, as shown in Fig. 1 (b), or after a long holding time of >1s. In contrast, a Gaussian fit fails to do so. Further confirmation on the use of the fit function comes from independent comparison with in-trap quantum Monte Carlo calculations for which satisfactory results are obtained for $U = 44\ t$ and $k_B T > 3\ t$ [25].

It is interesting to study samples after ramps which satisfy only the local adiabaticity condition, but are done more quickly than that presented Fig. 1 (b). Comparing profiles obtained from different speeds (Fig. 1 (a) and (b)), we can clearly see that locally adiabatic ramps do not guarantee global thermalization. We ask, in what manner is global equilibrium lost and reestablished? From Fig. 2 (d, e), we indeed find the fits do not simultaneously describe the flatness of the plateau, the density kink at $n = 1$, and the density tail, using a global set of thermodynamic parameters.

Our first step to study these non-equilibrated samples is to hold them in the lattice and monitor how they thermalize. To quantify the degree of thermalization, we compare the apparent temperatures in different parts of the sample, where local thermodynamic quantities are extracted by fitting the density profiles piecewise. Figure 4 shows an example of how two divisions of the sample may be fitted to determine the associated T and μ_c. Immediately after the standard ramping procedure ($V_f = 14\ E_r$, $\alpha < 0.7$), we find that the inner temperature $T_1 = 1.5$ nK is much lower than the outer shell $T_2 = 7.9$ nK. After an additional hold time of 1 s, the samples are much closer to full thermalization, that is to say, both temperatures and chemical potentials in different regimes come close to a common value.

The full evolution toward global thermal equilibrium is shown in Fig. 5. After the ramp, we hold the samples in the lattices for up to 1 s; we find it takes over 1 s for the inner and outer temperatures and chemical potentials to converge to $T \approx 9$ nK and $\mu_c \approx k_B \times 23$ nK. Note that the final temperature is still lower than the initial temperature of the superfluid of 20 nK. The thermalization process in the MI regime is much slower than the tunneling $t = \hbar/(16\text{ ms})$ and the radial confinement $\sqrt{\omega_x \omega_y} = 1/(14\text{ ms})$. This is likely because of the large sample size $L = \sqrt{N} d$ which requires a long thermalization time on the order of $\tau_{th} = (L/d)(\hbar/t)$. Indeed, $\tau_{th} = 1.6$ s for $N = 10,000$ is reasonably close to our observation.

Global cooling of a sample after the lattice ramp is an expected thermodynamical process. In 3D lattices, cooling of a trapped sample can occur isentropically [17, 18]. In 2D lattices, similar cooling is also probable. This cooling comes predominately from the change of the density of state across the SF-MI transition. Notably, however, our standard ramps are likely not globally isentropic; the

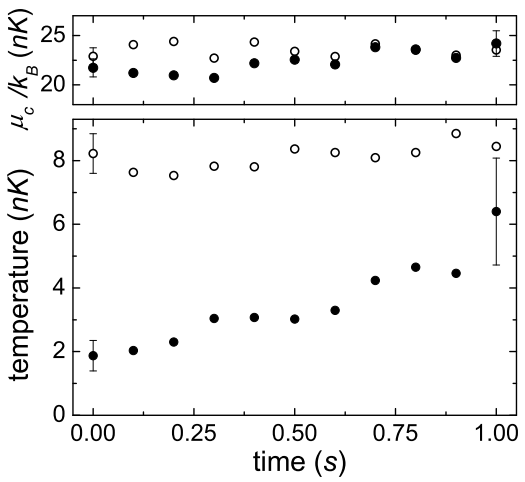

FIG. 5: Chemical potential and temperature of the sample after the standard ramp process. Sample preparation and the analysis are identical to those in Fig. 4. Chemical potentials and temperatures from the density fits are shown in the outer region ($r > 45d$, open circles) and the inner region ($r < 45d$, solid circles). Error bars show typical 1σ fitting uncertainty. Systematic heating due to the dipole trap and lattices is independently measured to be 0.8∼1.0 nK/s.

above theories might not apply well when a strong temperature gradient is developed.

The strong local cooling near the center of the sample is unexpected and intriguing. One possible process is the Joule-Thomson effect; a rapid expansion can quickly cool the sample. For quantum gases with weak interaction, the Joule-Thomson effect cools Bose gases and heats Fermi gases [26]. Detailed calculation is needed for quantitative comparison with our observation. A second possible process is associated with the vanishing of the critical temperature near the critical point. When a SF approaches the SF-MI transition, the critical temperature T_c drops to zero as density approaches the Mott lobe at $n = 1, 2..$ [4, 9]. As entropy of a Bose gas generally scales as $S = f(T/T_c)$ [27], a locally isentropic process can potentially cool the sample quickly near $n = 1$ when T_c vanishes. In principle this cooling can be balanced by the heating in the MI regime where the MI gap quickly rises [16], but a detailed theoretical study of non-equilibrium phenomena near the transition would be necessary to understand this fully.

In summary, we show that the *in situ* density profiles of atoms in 2D optical lattices provide a viable tool for determining thermodynamic quantities of the sample.

In the Mott insulator regime, it is possible to express the density profile analytically. When the lattice ramp is adiabatic with respect to the hopping, global thermalization is not necessary established. We observe both a very low temperature regime and slow dynamics toward thermal equilibrium. The local cooling process and slow rethermalization is possibly associated with the quantum phase transition. This cooling phenomenon provides interesting prospects to observe new quantum phases locally at lower thermal energy scales than might otherwise be achievable.

We thank T.L. Ho, J. Freericks, D.-W. Wang, R. Scalettar, Q. Zhou, and G. Mazenko for helpful discussions. This work is supported by NSF Award No. PHY-0747907 and under ARO Grant No. W911NF0710576 with funds from the DARPA OLE Program, and the Packard foundation. N.G. acknowledges support from the Grainger Foundation.

[1] I. Bloch, J. Dalibard, and W. Zwerger, Rev. Mod. Phys. **80**, 885 (2008).
[2] M. Lewenstein, A. Sanpera, V. Ahufinger, B. Damski, A. Sen and U. Sen, Adv. in Phys. **56**, 243 (2007).
[3] M. Greiner, O. Mandel, T. Esslinger, T. W. Hansch, and I. Bloch, Nature **415**, 39 (2002).
[4] M. P. A. Fisher, P. B. Weichman, G. Grinstein, and D. S. Fisher, Phys. Rev. B **40**, 546 (1989).
[5] D. Jaksch, C. Bruder, J.I. Cirac, C.W. Gardiner, and P. Zoller, Phys. Rev. Lett. **81**, 3108 (1998).
[6] R. Jördens, N. Strohmaier, K. Günter, H. Moritz, and T. Esslinger, Nature **455**, 204 (2008).
[7] U. Schneider, L. Hackermüller, S. Will, Th. Best, I. Bloch, T.A. Costi, R.W. Helmes, D. Rasch, A. Rosch, Science, **322**, 1520 (2008).
[8] J. Hubbard, Proc. R. Soc. London, Ser. A **276**, 283 (1963).
[9] S. Sachdev, "Quantum Phase Transitions", Cambridge Univ. Press, Cambridge, (1999).
[10] J. Zakrzewski, and D. Delande, Phys. Rev. A **80**, 013602 (2009).
[11] S.R. Clark and D. Jaksch, Phys. Rev. A **70** 043612 (2004).
[12] T. Gericke, F. Gerbier, A. Widera, S. Fölling, O. Mandel, and I. Bloch, J. of Mod. Op. **54**,735 (2007).
[13] F. Gerbier, S. Trotzky, S. Fölling, U. Schnorrberger, J. D. Thompson, A. Widera, I. Bloch, L. Pollet, M. Troyer, B. Capogrosso-Sansone, N. V. Prokof'ev, and B. V. Svistunov, Phys. Rev. Lett. **101**, 155303(2008).
[14] N. Gemelke, X. Zhang, C.L. Hung, and C. Chin, Nature **460**, 995 (2009).
[15] Y. Kato, Q. Zhou, N. Kawashima, and N. Trivedi, Nature Phys. **4**, 617 (2008).
[16] A. M. Rey, G. Pupillo, and J. V. Porto, Phys. Rev. A **73**, 023608 (2006).
[17] T.-L. Ho and Z. Qi, Phys. Rev. Lett. **99**, 120404(2007).
[18] F. Gerbier, Phys. Rev. Lett. **99**, 120405 (2007).
[19] T.-L. Ho and Q. Zhou, PNAS **106**, 6916 (2009).
[20] M. Popp, J.-J. Garcia-Ripoll, K. G. H. Vollbrecht and J. I. Cirac, New J. Phys. **8** 164 (2006).
[21] C.L. Hung, X. Zhang, N. Gemelke, and C. Chin, Phys. Rev. A **78**, 011604(R) (2008).
[22] I. B. Spielman, W. D. Phillips, and J. V. Porto, Phys. Rev. Lett. **100**, 120402 (2008).

[23] B. Capogrosso-Sansone, Ş.G. Söyler, N. Prokofev, and B. Svistunov, Phys. Rev. A **77**, 015602 (2008).
[24] R. Scalettar, private communication.
[25] D.-W. Wang, private communication.
[26] D.-Q. Yuana and C.-J. Wang, Phys. Lett. A, **363**, 487 (2007).
[27] L. D. Carr, G. V. Shlyapnikov, and Y. Castin, Phys. Rev. Lett. **92**, 150404 (2004).